Changes in the high latitude Southern Hemisphere through the Eocene-Oligocene Transition: a model-data comparison

Alan T. Kennedy-Asser[1,2], Daniel J. Lunt[1,2], Paul J. Valdes[1,2], Jean-Baptiste Ladant[3], Joost Frieling[4], Vittoria Lauretano[2,5]

[1] BRIDGE, School of Geographical Sciences, University of Bristol, Bristol, UK
[2] Cabot Institute for the Environment, University of Bristol, Bristol, UK
[3] Department of Earth and Environmental Sciences, University of Michigan, Ann Arbor, USA
[4] Marine Palynology and Paleoceanography, Laboratory of Palaeobotany and Palynology, Department of Earth Sciences, Faculty of Geosciences, Utrecht University, Princetonlaan 8a, 3584CB Utrecht, the Netherlands
[5] Organic Geochemistry Unit, School of Chemistry, University of Bristol, Bristol, UK

Correspondence to: Alan T. Kennedy-Asser (alan.kennedy@bristol.ac.uk)

Abstract. Global and regional climate changed dramatically with the expansion of the Antarctic Ice sheet at the Eocene-Oligocene Transition (EOT). These large-scale changes are generally linked to declining atmospheric pCO_2 levels and/or changes in Southern Ocean gateways such as the Drake Passage around this time. To better understand the Southern Hemisphere regional climatic changes and the impact of glaciation on the Earth's oceans and atmosphere at the EOT, we compiled a database of sea and land surface temperature reconstructions from a range of proxy records and compared this with a series of fully-coupled climate model simulations. Regional patterns in the proxy records of temperature show that cooling across the EOT was less at high latitudes and greater at mid-latitudes. Climate model simulations have some issues in capturing the zonal mean latitudinal temperature profiles shown by the proxy data, but certain simulations do show moderate-good performance at recreating the temperature patterns shown in the data. When taking into account the absolute temperature before and after the EOT, as well as the change in temperature across it, simulations with a closed Drake Passage before and after the EOT or with an opening of the Drake Passage across the EOT perform poorly, whereas simulations with a drop in atmospheric pCO_2 in combination with ice growth generally perform better. This provides further support to previous research that changes in atmospheric pCO_2 are more likely to have been the driver of the EOT climatic changes, as opposed to opening of the Drake Passage.

1 Introduction

Global cooling and significant expansion of glacial ice over Antarctica at the Eocene-Oligocene Transition (EOT), ~33.7 million years ago (Ma; Zachos et al., 2001; Coxall et al., 2005), would have potentially resulted in large but uncertain changes in the Southern Ocean and the climate of the high latitude Southern Hemisphere (Bohaty et al., 2012; Passchier et al., 2013). Numerous palaeoclimate modelling studies have shown that changes in Antarctic ice sheet extent, atmospheric pCO_2 levels and palaeogeographic reconstruction around this period of the Earth's history can all impact on the modelled global and/or

regional climate (Goldner et al., 2014; Knorr & Lohmann, 2014; Kennedy et al., 2015). Interestingly, all of these studies show some areas of warming in the Southern Ocean in response to the imposition of an Antarctic ice sheet in the model, but the different models find the warming to occur in different regions. Recent modelling work using an ensemble of simulations from the model HadCM3BL (Kennedy-Asser et al., 2019) showed that, for at least that particular climate model, the sea surface

5 temperature response is particularly uncertain in high latitude regions due to uncertainties in the model boundary conditions that could potentially be exaggerated due to incomplete model spin-up.

While global circulation models (GCMs) are useful tools for testing our understanding of the Earth system, their inherent uncertainty within this region shows that it is necessary to integrate proxy evidence to build up a more robust picture of Southern Ocean changes across the EOT. To this end, here we compile a large multi-proxy database of temperature for the

10 high latitude Southern Hemisphere, incorporating a multitude of different proxy records in terms of methods, sites and temporal coverage. Despite sometimes not being directly comparable, the inclusion of very different kinds of proxy evidence provides both qualitative and quantitative measures against which model simulations can be compared and evaluated. The quantitative elements of the dataset can also be used to describe general temperature patterns (e.g. in terms of the regional mean or latitudinal gradient), and model simulations that perform relatively well can then be used in conjunction with the proxy dataset

15 to start to explain what changes may have occurred in this region across the EOT.

Proxy records of past climate and the 'equilibrium' climate simulations generally performed for the EOT both have strengths and weaknesses. Proxy records, specifically sediment cores, are particularly good for reconstructing the temporal domain of past climate, showing changes through long time periods at a particular point in space (e.g. Zachos et al., 2001). By contrast, complex fully-coupled climate models generally cannot be run for long transient simulations and instead only provide

20 equilibrium snapshots of climate at a single point in time but offer a complete spatial picture of how different regions compare to one another in a physically consistent way (e.g. Lunt et al., 2016).

The aim of this data synthesis is to create proxy datasets that are comparable to model simulations, i.e. can be used to validate the models in the spatial domain. This necessitates reducing the temporal variability of the proxy data into broad time slices,

25 which was done for late Eocene absolute conditions (generally 36.4-34.0 Ma), relative changes across the EOT and early Oligocene absolute conditions (generally 33.2-32.0 Ma). Dictated by the nature and inherent uncertainties in the age models associated with the proxy data, the definition of the time slices remains reasonably crude. Indeed, proxy records used will be on different age models at each locality and cover somewhat different periods and lengths of time. This introduces an element of uncertainty; it has been shown that there was variability in the few million years either side of the Eocene-Oligocene

30 Boundary (E/O; e.g. Coxall & Pearson, 2007; Scher et al. 2014; Galeotti et al. 2016). Time averaging approximately two million years prior to and after the E/O will potentially average out this temporal variability (if a long record for a particular location is available) or potentially skew results (if for example a short-term excursion is captured in the record). However,

the time averaged records should be more representative of the average climate state at a given locality, therefore making the proxy records of use for the model validation.

Two specific research questions are addressed in this paper. Firstly, what are the spatial patterns of temperature change inferred from proxy records for the high latitude Southern Hemisphere before, after, and across the EOT? Secondly, which GCM
5 boundary conditions give the best fit to the range of qualitative and quantitative proxy records of temperature before, after, and across the EOT?

A brief overview of the data synthesis, model simulation details and evaluation methods follow in Section 2. Section 3 presents the results of the model-data comparison. Finally, Sections 4 and 5 discuss the significance of the results and the potential scope of future research respectively.

2 Methods

2.1 Data synthesis

Many different proxy records for in-situ sea surface temperature (SST) are available. These include quantitative records using stable isotopes and trace metals ($\delta^{18}O$ and Mg/Ca; Bohaty et al., 2012), clumped isotopes (Δ_{47}; Petersen & Schrag, 2015) and
15 organic biomarkers (TEX$_{86}$ and U$^{K'}_{37}$; e.g. Liu et al., 2009). Quantitative proxies can be used in conjunction with qualitative records, such as nannofossil or dinoflagellate species assemblage and size (e.g. Villa et al., 2013; Houben et al., 2013), to provide further evidence for temperature ranges or relative changes where or when quantitative data might be sparse. For example, the dinoflagellate species *S. antarctica*, broadly suggests colder temperatures with higher abundance, while its presence suggests mean annual SSTs < 10 °C (Zonnefeld et al., 2013), even if spatial integration of microfossils is taken into
20 account (Nooteboom et al. 2019).

Some terrestrial surface air temperature (SAT) records are also available, such as those derived from clay weathering products (S-index; e.g. Passchier et al., 2013) and from vegetation reconstructions (based on Nearest Living Relative, NLR, e.g. Francis et al., 2009; or the Coexistence Approach, e.g. Pound & Salzmann, 2017). These records may or may not be in-situ (in time or space), with clay weathering products for example having been exported from terrestrial regions to where they are deposited
25 in ocean sediment cores.

These proxies respond to the climate system in different ways and all rely on various assumptions, resulting in uncertainty ranges that can be incorporated into the model-data comparison. Some proxies provide continuous quantitative data that can be directly compared to models or other records, e.g. absolute temperature estimates. Other proxies may provide ordinal

(qualitative) data; that is, data that can be ranked into an order of greater or lesser magnitude but from which absolute values are not attainable. Both of these kinds of data can be used to evaluate the palaeoclimate model simulations.

Values and data are compiled from a range of sources within published material. Ideally, the data is taken from the supplementary material of the related papers. In other cases, mean values might be quoted in tables, figures or in the text of

5   papers; however, it can be unclear over what time period these means are taken or how uncertainty values are calculated. Although this is not the most accurate way of obtaining data, in some cases this might provide the only data available and so still warrants inclusion. The sources of all data points used are outlined in detail in the supplementary information (Tables S1-3), a digital version of which can also be accessed through the Open Science Framework (Kennedy-Asser, 2019).

10 Uncertainty in the proxy data records could arise due to calibration uncertainties or could be due to temporal variability in the record (particularly the case here where temporal means are taken for each time slice). These various aspects make it challenging to rigorously define and quantify uncertainty. Generally, uncertainty is taken as the published values where available. Alternatively, generalised calibration uncertainty for a given proxy (if known) or two standard deviations of the temporal variability in the records can be taken as the uncertainty. Some records are presented in terms of annual temperature

15 range and these limits can be taken as the uncertainty around the annual mean (assumed to be the mean of the maximum and minimum of the range). The source of the uncertainty ranges used are also detailed in the supplementary material of this paper (Tables S1-3) and Kennedy-Asser (2019).

Some studies (e.g. Dowsett et al., 2012; Pound & Salzmann, 2017) devise semi-quantitative metrics for the quality of proxy

20 records, based upon factors such as preservation, dating quality, calibration errors etc. when compiling their datasets. Here, there is no formal assessment of the quality of individual proxies or records, nor is there any reinterpretation or recalculation of existing datasets, as this would beyond the scope of the paper. Instead, here the dataset integrates as many independent proxies as possible for each site, and all are used to evaluate the model simulations. It is important to note that the same proxy is only used in the compilation once per site per time slice. If two or more records using the same proxy at the same site are

25 available, generally the most recent value in the literature is used (e.g. Passchier et al., 2013 and 2016 both provide estimates for temperature using the S-index in Prydz Bay, so the 2016 value is used). Different proxies are weighted equally in the model evaluation, with sites where there are multiple records therefore being weighted more strongly for the purpose of model-data comparison.

30 In total, data were taken from 14 sites, ranging in palaeolatitude from 53 to 77 °S and palaeolongitude from 63 °W to 177 °E. The compiled temperature records are shown for the late Eocene and for the early Oligocene in Figure 1, and for the change across the EOT in Figure 2. The references for all data points are included in the supplementary information.
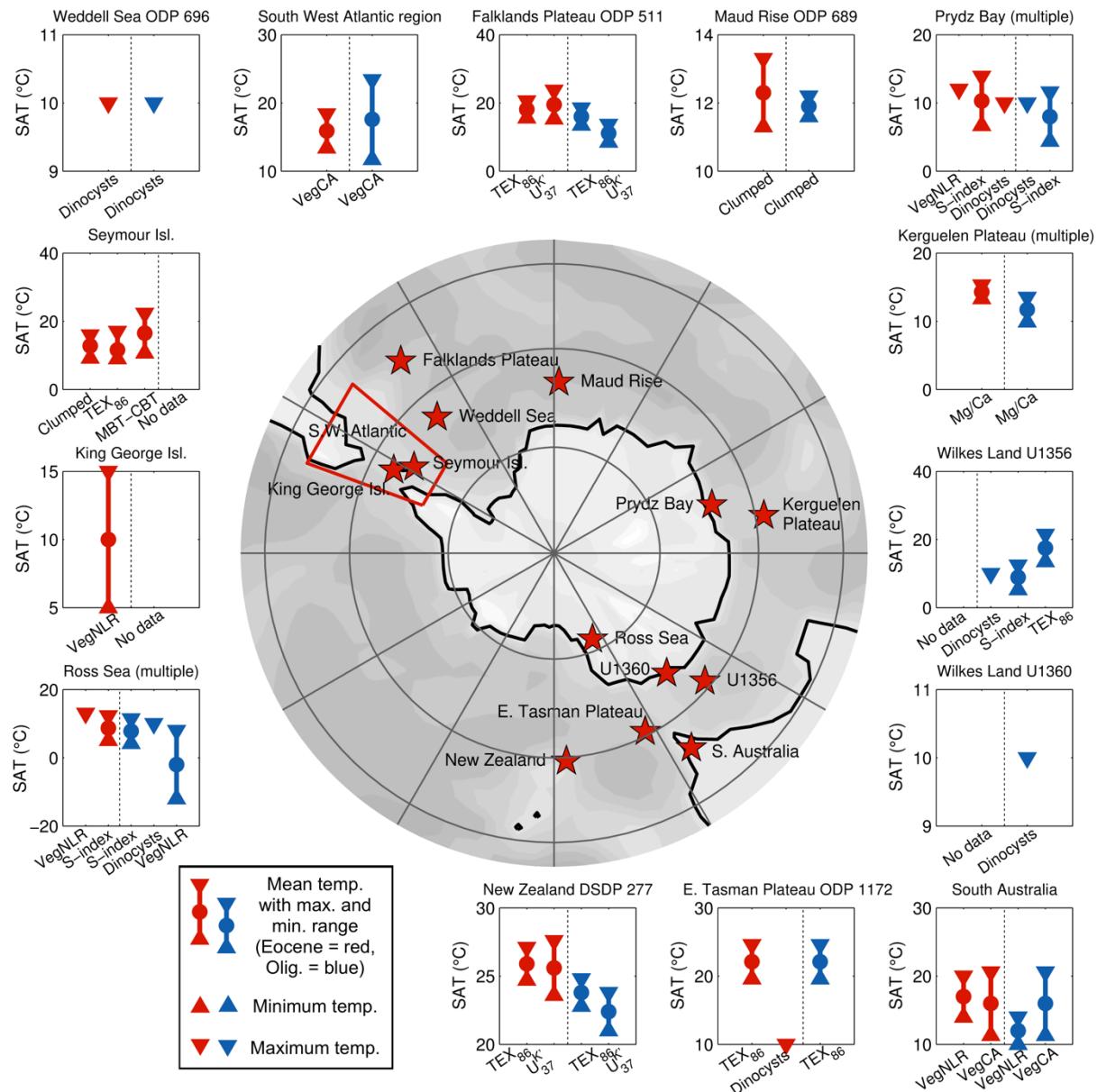
Figure 1: Mean annual temperature (°C) from proxy records for all sites during the late Eocene and early Oligocene. The mean values (circles) are shown with maximum and minimum values (error bars), while ordinal limits are shown by upwards (greater than) or downwards (less than) pointing triangles. Late Eocene records are in red and early Oligocene records in blue.
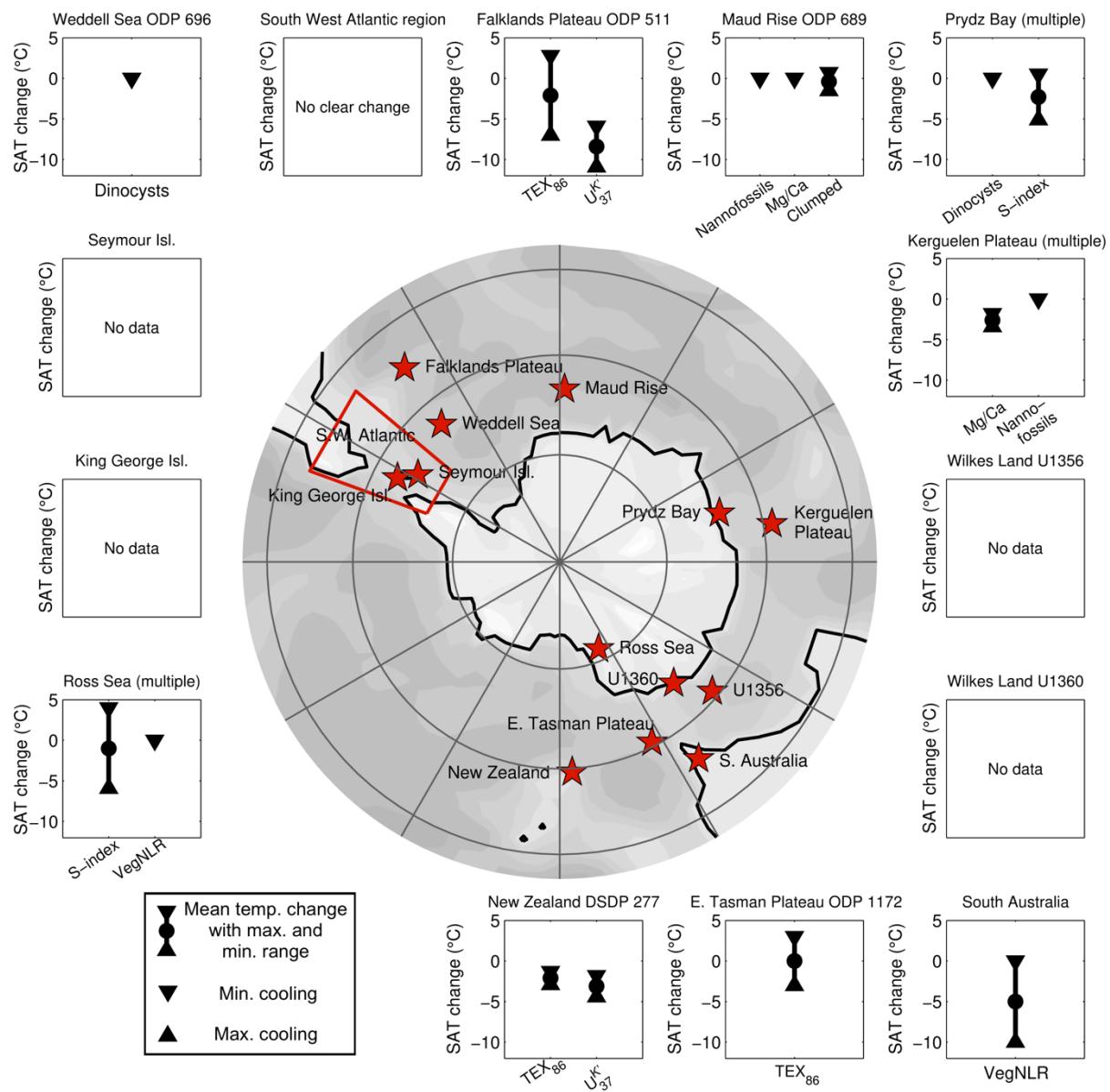
Figure 2: Changes in mean annual temperature (°C) from proxy records for all sites across the EOT. The mean values (circles) are shown with maximum and minimum values (error bars), while ordinal limits are shown by upwards or downwards pointing triangles.

2.2 Model simulations

The proxy datasets compiled here are compared to the fully spun-up HadCM3BL-M2.1aE simulations outlined in Kennedy-Asser et al. (2019) and simulations from FOAM outlined in Ladant et al. (2014). A detailed description of the models' setup
5   and the simulation details can be found in the respective references. These models are all relatively low resolution and are less complex than some others that have been used in recent studies (e.g. Hutchinson et al., 2018; Baatsen et al., 2018); however, they are still regularly used in palaeoclimate research of this period. An overview of the simulations used is provided in Table 1.

10   **Table 1: Brief overview of climate models and the boundary conditions varied for each.**

Model	Atmos. resolution	Ocean resolution	No. of simulations used	Simulation length (years)	Palaeogeog. vars.	Ice sheet vars.	pCO_2 vars. (ppmv)	Reference
HadCM3BL-M2.1aE	96x73x19	96x73x20	8	>6,000	Open Drake Passage	No ice	840 / 560	Kennedy-Asser et al., 2019*
					Open Drake Passage	EAIS	840 / 560	
					Closed Drake Passage	No ice	840 / 560	
					Closed Drake Passage	EAIS	840 / 560	
FOAM	48x40x18	128x128x24	6	2,000	Open Drake Passage	No ice	1,120 / 840 / 560	Ladant et al., 2014†
						Small EAIS	560	
						EAIS	560	
						Full AIS	560	

*_HadCM3BL simulations are those from the 'Spin-up ensemble' in Kennedy-Asser et al. (2019), which were selected as they are more adequately spun-up. These have a present-day orbital configuration._

†_FOAM simulations are those with a present-day orbital configuration: other orbital configurations from Ladant et al. (2014) were not tested._

In order to evaluate against the proxy dataset of relative changes across the EOT, pairs of model simulations can be selected that represent the forcing changes occurring across the EOT. These pairs of model simulations represent a before and an after state, with the difference in the boundary conditions between the pairs described as the forcing and the difference in the modelled climate representing the change across the EOT. The model-data comparison in Kennedy-Asser et al. (2019) was reasonably idealised in that mostly isolated changes in the model setup were taken as the forcing across the EOT; for example, a change in palaeogeography but no change in pCO$_2$ or ice sheet extent. Given that the vast majority of glaciological proxy data gives evidence of glacial expansion, here the modelled forcing must include some sort of ice expansion (i.e. the early Oligocene simulation must contain an ice sheet and the late Eocene simulation must contain no ice sheet). The simulation pairs may additionally include other forcing changes that are potentially relevant to describe the state of the Earth system before and after the EOT, namely pCO$_2$ level and gateway configuration. Simulation pairs were chosen that represented:

- An expansion of ice over Antarctica from an ice-free state to either an EAIS of full AIS, with all other boundary conditions remaining the same
- A similar expansion of ice over Antarctica but also combined with a simultaneous drop in pCO$_2$, with palaeogeographic boundary conditions remaining the same
- A similar expansion of ice over Antarctica but also combined with a simultaneous change in palaeogeography (an opening of the Drake Passage), with pCO$_2$ boundary conditions remaining the same
- A similar expansion of ice over Antarctica but also combined with a simultaneous change in palaeogeography (an opening of the Drake Passage) and a drop in pCO$_2$

This produced 9 pairs of simulations from HadCM3BL and 9 pairs from FOAM. A detailed description of all simulations and simulation pairs used is included in Table S4 of the supplementary material.

2.3 Metrics of comparison

At each site where proxy data is available, the modelled temperature is taken as the mean over a three by three grid cell area surrounding each proxy location, with the maximum and minimum modelled temperature also taken from these nine grid cells as the modelled uncertainty. The principal method used to evaluate the GCMs against the proxy dataset is the root mean square error (RMSE), which simply finds the mean difference between the models and the data for all comparable points. The RMSE is calculated in two ways:

Firstly, the 'standard' RMSE, defined in Eq. (1), is calculated from the maximum or minimum of the uncertainty range of the proxy data to the minimum or maximum of the uncertainty range in the model (if the model is too warm or cold, respectively).

$$standard\ RMSE = \sqrt{\frac{\sum_n^i E_{S,i}^2}{n}}, \tag{1}$$

Where, E_S is the error, defined in Eq. (2), and n is the number of proxy records for a given time slice.

$$E_{S,i} = T_{p,i} - T_{m,i}, \tag{2}$$

Where T_p is the range of temperatures indicated by proxy reconstruction i and T_m is the range of temperatures indicated by a
5 model simulation for the location of record i. The standard error, E_S, is taken as zero if the range of model uncertainty, T_m, overlaps the range of proxy uncertainty, T_p. This can be calculated for continuous data or ordinal data that provides an upper range for the temperature, such as the presence of *S. antarctica*. Examples of how this is applied are illustrated in Supplementary Figure 1.

10 Secondly, the RMSE is calculated once the mean temperature of all data points/sites (either in the proxy dataset or for a given model simulation) has been removed. The purpose of removing the mean is so the model performance is not primarily judged against systematic warm or cold biases, which are typical at high latitudes (Huber & Caballero, 2011; Lunt et al., 2012). This 'normalised' RMSE, defined in Eq. (3), instead evaluates the spatial pattern of temperature in the Southern Ocean. This metric is used with continuous data where a mean value is available, again with the error taken between the ranges of the proxy and
15 model uncertainty.

$$normalised\ RMSE = \sqrt{\frac{\sum_n^i E_{N,i}^2}{n}}, \tag{3}$$

Where, E_N is the error of the normalised data, defined in Eq. (4).

$$E_{N,i} = (T_{p,i} - \overline{T_p}) - (T_{m,i} - \overline{T_m}), \tag{4}$$

Where $\overline{T_p}$ is the mean temperature of all proxy records and $\overline{T_m}$ is the mean modelled temperature across all proxy record sites.

'Count metrics' can also be used for the absolute and relative change data comparisons, allowing a large range of proxy records to be incorporated. These metrics count how many of the data points the model is consistent with in terms of magnitude (i.e. within the error bars of) and, for the change across the EOT, the number of records for which the model simulations correctly predict the direction of change. This can allow ordinal data (such as increasing cold water taxa) to contribute to the comparison.

In order to assess the simulations across multiple criteria, metric scores that have comparable units (e.g. the two RMSE metrics) can simply be summed or averaged. Additionally, to further expand upon the idealised model-data comparison of Kennedy-Asser et al. (2019), it is important to consider not just if the simulated change across the EOT is realistic, but also if the starting and ending state are realistic compared to the late Eocene and early Oligocene datasets. This is done by combining the metric
30 scores for a pair of simulations that describe the change across the EOT (compared to the EOT dataset) with metric scores for

the pre- and post-EOT simulations that make up that pairing (compared to the late Eocene and early Oligocene datasets). If the datasets had a consistent spatial coverage for each of the time slices, the difference between the late Eocene and early Oligocene absolute datasets would be the same as the EOT relative change dataset. However, because there are some sites with records available only before or after the EOT, and some relative changes for which absolute values are not available, the pair of

5 simulations that gives the best fit before and after the EOT is not necessarily the same pair as gives the best fit for the observed change across the EOT. Which metric is used to evaluate across the time slices, and if there is any weighting put on the absolute or relative change datasets, is subjective. Although the count metrics are shown for reference, here, the combined rank score for each time slice is based upon only the two RMSE metrics and the three time slices (late Eocene, early Oligocene and EOT) are weighted equally.

2.4 Benchmarks for evaluation

For the model simulations to be described as performing particularly 'well' or 'poorly', it is necessary to have some sort of

15 benchmark to compare the models' performance against. For the three time slices, two benchmarks are used: these can be thought of as hypothetical generalisations of the whole regional high latitude Southern Hemisphere climate based only upon proxy data. First, the mean temperature (or temperature change) of all sites and proxies is taken as a homogeneous value at all sites. Second, the ordinary least squares linear fit through the mean temperatures (or temperature change) with palaeolatitude from all proxies and sites, shown in Figure 3, is taken to produce a synthetic, latitudinally varying temperature field for the

20 region. If model simulations perform better than both benchmarks, they can be described as showing *good* performance as they are correctly modelling zonal and regional variation beyond this general latitudinal trend. If the simulations perform worse than both benchmarks, they show *poor* performance and are failing to identify even the most basic variation in the dataset. If the simulations outperform the constant mean benchmark but not the latitudinal gradient benchmark, they are described as showing *moderate* performance. When evaluating the model simulations across both RMSE metrics, if a simulation out

25 performs a benchmark for one metric but not the other, its performance can be described for example as *moderate-poor*.

3 Model-data comparison

3.1 Latitudinal temperature profiles

30 The regional mean of the proxy records and latitudinal temperature gradient benchmarks are shown in Figure 3 along with the best HadCM3BL and FOAM simulations identified in Section 3.5. The absolute temperature profiles in the late Eocene and early Oligocene proxy datasets show colder temperatures at higher latitudes than mid-latitudes, as would be expected. The latitudinal gradient is steeper in the early Oligocene (0.54 °C °N^{-1}) compared to the late Eocene (0.49 °C °N^{-1}). The change in

temperature across the EOT identified by the proxies has a negative slope, suggesting that cooling is greater at mid-latitudes and is less at higher latitude sites, which could reflect a qualitative agreement with modelling results (Goldner et al., 2014; Knorr & Lohmann, 2014; Kennedy et al., 2015; Kennedy-Asser et al., 2019), where the heterogeneous temperature response in the models saw some high latitude areas warming (or cooling less). The steepness of the gradient for the EOT dataset (-0.20

5 °C °N^{-1}) is enhanced by the strong cooling at the lower latitude Falklands Plateau; however, even if this site were to be omitted from the fit, the latitudinal gradient would still be negative (-0.14 °C °N^{-1}; figure not shown). Implications of this latitudinal gradient change across the EOT will be discussed further in Section 4.2.
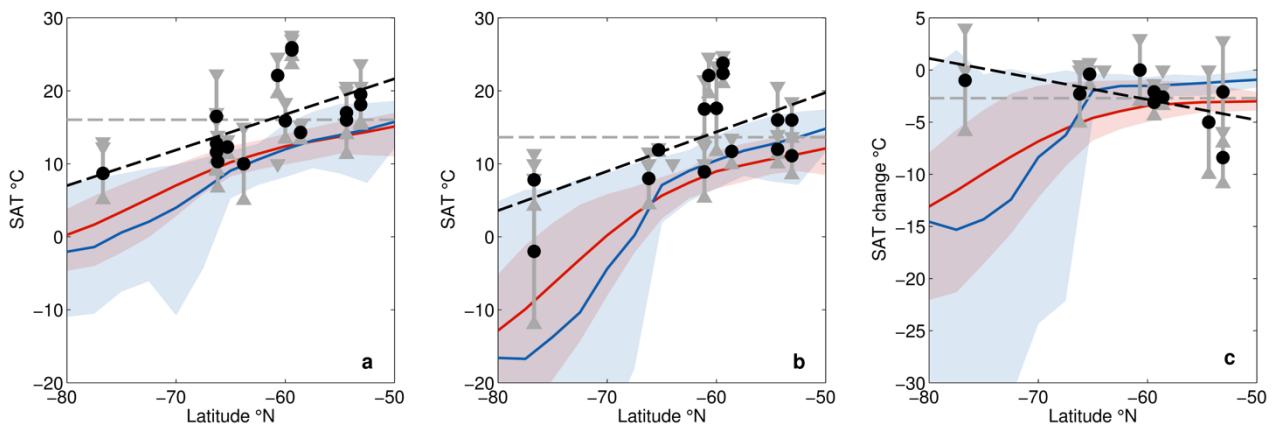
10 **Figure 3: Latitudinal profiles of a) late Eocene absolute temperature, b) early Oligocene absolute temperature and c) EOT temperature change from proxy records. The regional mean values are plotted in grey dotted lines and latitudinal gradients (calculated using ordinary least squares) in black dotted lines. Circles show proxy data mean values, while their uncertainty ranges and maximum/minimum limits are shown by the bars and triangles. The coloured lines show the zonal mean surface air temperature profile for the best HadCM3L (blue) and FOAM (red) simulations, with the**

15 **shading showing the zonal maximum and minimum surface air temperature for each model.**

3.2 Late Eocene temperatures

The standard RMSE, normalised RMSE and count metric for all of the ice-free simulations and the benchmarks in comparison to the late Eocene dataset are shown in Figure 4a. The standard RMSE scores show that absolute temperature biases are in

20 general large compared with the benchmarks. The standard RMSE scores are better for simulations at higher pCO_2 levels for both HadCM3BL and FOAM, showing there is a cold bias in the simulations from both models. As a result, only one HadCM3BL simulation outperforms the homogeneous benchmark (3x pre-industrial pCO_2 levels and an open Drake Passage). No simulations from either model outperform the latitudinal gradient benchmark in terms of the standard RMSE.
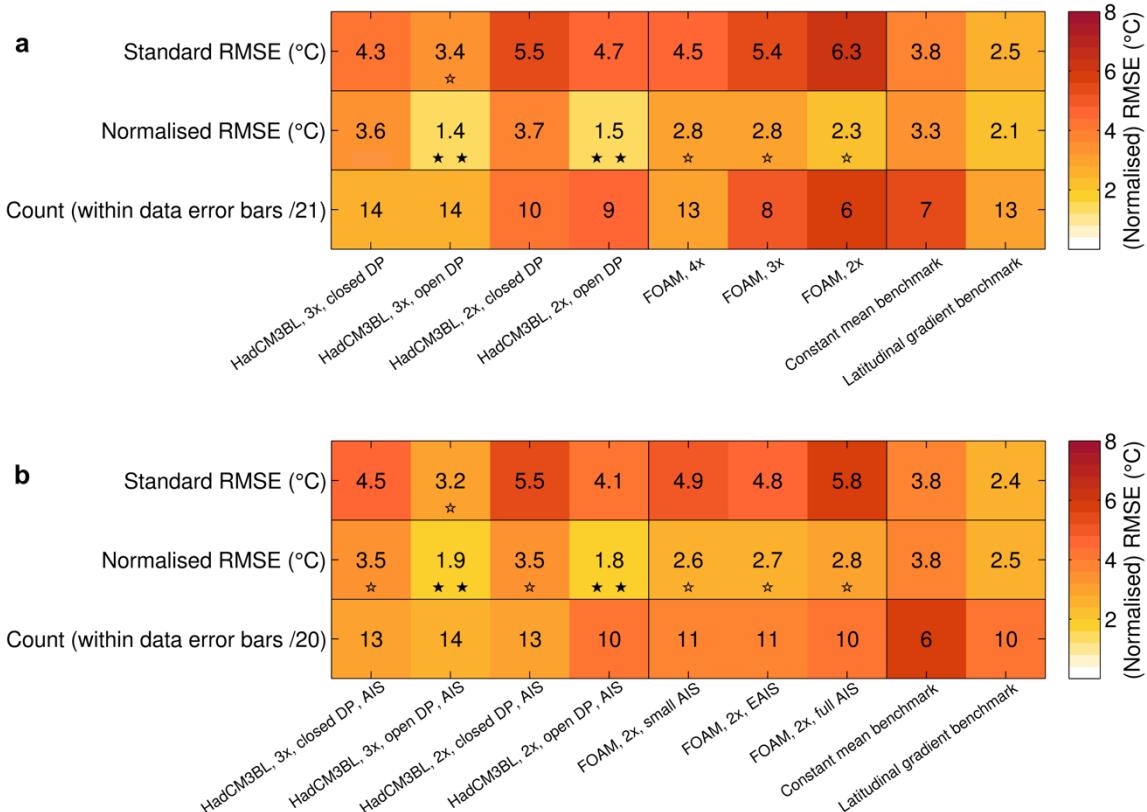
Figure 4: Standard RMSE (°C), normalised RMSE (°C) and count metric for all ice free model simulations and the benchmarks compared against the late Eocene dataset (a) and the early Oligocene dataset (b). Labels on the x-axis refer to the pCO_2 level ('2x', '3x' or '4x' pre-industrial levels), state of the Drake Passage ('DP') in HadCM3BL simulations and the size of the Antarctic ice sheet (AIS) in FOAM simulations. The colour scale of the count metric is normalised to match that of the RMSE metrics (i.e. white = best: all sites are within error bars; dark orange = worst: no sites are within error bars). For a given metric, single open stars indicate simulations with *moderate* performance and double black stars indicate simulations with *good* performance.

When the mean temperature bias is removed for the normalised RMSE, more of the simulations outperform the constant mean benchmark and some outperform the latitudinal gradient benchmark. For FOAM, with the cold temperature bias removed, the lower pCO_2 simulation performs better than the higher pCO_2 simulations and all outperform the constant mean benchmark. The best simulations are those from HadCM3BL with an open Drake Passage, which perform better than the latitudinal gradient benchmark. The worst simulations are the HadCM3BL simulations with a closed Drake Passage, both of which fail to outperform either benchmark, suggesting this palaeogeographic configuration has a major influence on the spatial patterns of temperature and is unrealistic.

No simulations outperform both benchmarks for both RMSE metrics, so none can be described as *good* by our definition. However, the HadCM3BL simulation at 3x PI pCO_2 with an open Drake Passage outperforms the homogenous benchmark for both metrics and the latitudinal gradient benchmark for the normalised RMSE, so can be described as *moderate-good*.

3.3 Early Oligocene temperatures

Figure 4b shows the standard RMSE, normalised RMSE and count metric for all glaciated simulations against the early Oligocene dataset. Again, there is a general cold bias indicated by the poorer standard RMSE scores for the lower pCO_2 simulations for HadCM3BL. Generally, the standard RMSE values are similar or slightly better compared to the late Eocene comparison. Again, only one simulation outperforms the constant mean benchmark: HadCM3BL at 3x pre-industrial pCO_2 with an open Drake Passage, with no simulations outperforming the latitudinal gradient benchmark for this metric. The FOAM simulation with the largest ice sheet configuration has a poorer RMSE compared to the FOAM simulations with smaller ice sheets, likely due to the cooling (and hence cold bias) being greater with a larger ice sheet.

For the normalised RMSE, all simulations outperform at least one benchmark. The HadCM3BL simulations with an open Drake Passage at either pCO_2 level are the joint best. Again, as with the late Eocene temperature data, the HadCM3BL simulations with the closed Drake Passage perform much worse than the equivalent open Drake Passage simulations in terms of the both RMSE metrics. Again for this metric, the FOAM simulation with the largest AIS does not perform as well as those with smaller ice sheet configurations (although the difference is not so marked). This suggests the AIS expansion across the EOT might not be at the upper range of volume estimates suggested by other studies (e.g. Bohaty et al., 2012; Wilson et al., 2013). Like for the late Eocene, no simulation can be described as *good* for both RMSE metrics; however, the glaciated HadCM3BL simulation at 3x pre-industrial pCO_2 with an open Drake Passage can be described as *moderate-good*.

3.4 EOT temperature change

All pairs of model simulations representing the change that occurred across the EOT are shown in Figure 5. It is important to note that, generally, the uncertainties in the EOT dataset are much greater relative to the magnitude of change, compared to the uncertainties relative to the absolute values in the late Eocene and early Oligocene datasets. As a result, the latitudinal gradient benchmark provides a remarkably good fit for the data covering the EOT, lying almost entirely within the data uncertainty. No model simulations perform as well as this benchmark, but again, because the uncertainty in the change relative to its magnitude is greater than in the absolute datasets, generally the model RMSE scores are lower for this dataset than the late Eocene or early Oligocene datasets.

Three HadCM3BL simulation pairs outperform the constant mean change benchmark for the standard RMSE metric: those with an open Drake Passage in response to AIS growth and a pCO_2 drop and those with a closed Drake Passage in response to AIS growth at both pCO_2 levels. No simulation pairs outperform the either benchmark for the normalised RMSE metric.
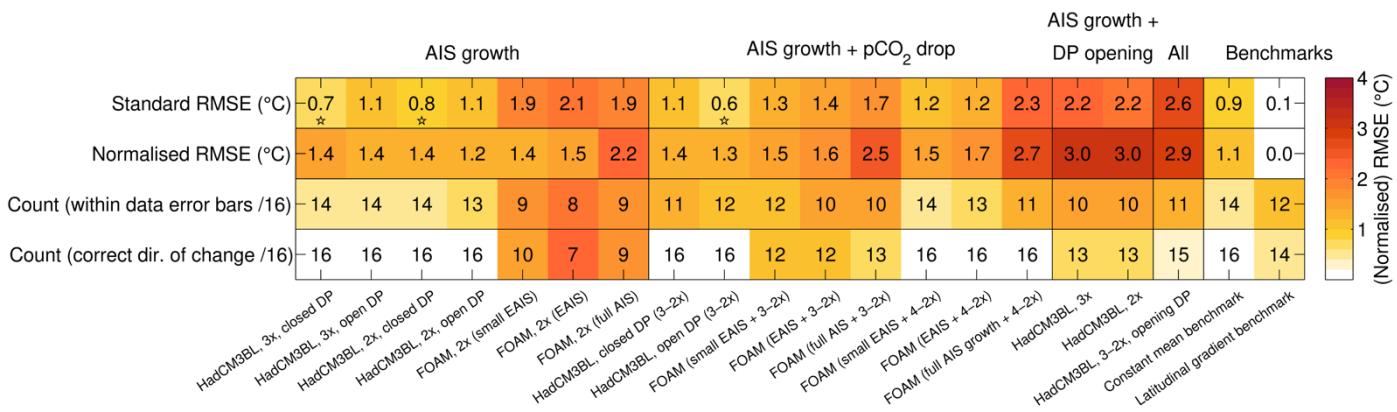
Figure 5: Standard RMSE (°C), normalised RMSE (°C) and count metrics for all pairs of model simulations representing the forcing across the EOT and the benchmarks compared against the EOT dataset. The simulation pairs are grouped by forcing. Labels on the x-axis refer to the pCO_2 level ('2x', '3x' or '4x' pre-industrial levels) and state of the Drake Passage ('DP'); brackets in the labels specify the size of AIS added or magnitude of pCO_2 drop. The colour scales of the count metrics are normalised to match that of the RMSE metrics and stars indicate _moderate/good_ performance as in Figure 4.

In contrast to what was shown for the absolute temperature dataset comparisons for the late Eocene and early Oligocene, the HadCM3BL simulation pairs with a closed Drake Passage (both before and after the EOT) perform relatively well, particularly for the standard RMSE. This shows that although simulations can be far from the proxies in absolute terms, they can still produce promising results in other ways. Similar to what was shown for the late Oligocene, the FOAM simulations generally fit the dataset best in terms of the standard and normalised RMSE when they have smaller ice sheets added. Although it makes little difference for the normalised RMSE scores, FOAM simulations which combine a pCO_2 drop in tandem with AIS growth perform better in terms of the standard RMSE and the count metrics (i.e. the number of sites which lie within error bars or simulate the correct direction of change) than those with which simulate only AIS growth.

Generally in terms of the forcings across all model simulation pairs, the AIS growth forcing in isolation produces the best normalised RMSE and performs comparably to the combined AIS growth and pCO_2 drop forcing in terms of the standard RMSE. For HadCM3BL, the AIS growth forcing produces better results for the count metric of sites within the data error bars whereas for FOAM the combined AIS growth and pCO_2 drop forcing produces better results for the count metrics. The HadCM3BL simulations with an opening of the Drake Passage (in combination with AIS growth or AIS growth and pCO_2 drop) generally gives the poorest fit for the RMSE metrics of all the simulation pairs and the worst count metric results of all

HadCM3BL simulation pairs. This suggests that opening of the Drake Passage across the EOT is the least likely of these model scenarios.

No simulations from any model perform better than either benchmark for both RMSE metrics, with the best HadCM3BL simulation pairing (with an open Drake Passage in response to both AIS growth and pCO$_2$ drop) coming the closest (its

5 normalised RMSE being 0.24 °C worse than the constant mean benchmark). All simulation pairs can therefore only be described as *moderate-poor* or *poor*. The reasoning for this poor performance is discussed further in Section 4.

3.5 Evaluation across time slices

As noted in Section 2.3, it is possible to evaluate the model simulations and model simulation pairs across various metrics.

10 The best five simulations (or simulation pairs) for the late Eocene, early Oligocene and for the change across the EOT based on the mean of their two RMSE metrics are shown in Table 2, along with the mean of the two RMSE metrics for each of the benchmarks for comparison. As well as taking the average RMSE for each time slice, the average RMSE can be taken across all three time slices. It is not always the case that simulation pairs that perform well for the observed EOT change also perform well when the late Eocene and early Oligocene data are incorporated. As was noted in Sections 3.1 and 3.2, for the absolute

15 temperatures, simulations with a closed Drake Passage perform relatively poorly. As a result, when the combined ranked performance score is calculated across all three time slices, the pairings with a closed Drake Passage are not found to perform as well, highlighting the importance of incorporating the absolute values into this model-data comparison. Again, this suggests that the Drake Passage was open prior to the EOT and the late Eocene. The best five simulations in terms of the mean standard RMSE and normalised RMSE across all three time slices are also listed in Table 2, along with the benchmarks for comparison.

Table 2: The five highest ranked simulations (or simulation pairs) in terms of mean standard and normalised RMSE for each time slice and across all three time slices.

Rank	Mean RMSE (°C)	Model	pCO_2 (ppmv)	AIS state	Drake Passage
			Late Eocene absolute		
	2.28		Latitudinal gradient benchmark		
1	2.42	HadCM3BL	840	No ice	Open
2	3.08	HadCM3BL	560	No ice	Open
	3.56		Constant mean benchmark		
3	3.64	FOAM	1,120	No ice	Open
4	3.93	HadCM3BL	840	No ice	Closed
5	4.12	FOAM	840	No ice	Open
			Early Oligocene absolute		
	2.49		Latitudinal gradient benchmark		
1	2.54	HadCM3BL	840	EAIS	Open
2	2.99	HadCM3BL	560	EAIS	Open
3	3.74	FOAM	560	EAIS	Open
4	3.77	FOAM	560	Small EAIS	Open
	3.79		Constant mean benchmark		
5	4.01	HadCM3BL	840	AIS*	Closed
			EOT change		
	0.05		Latitudinal gradient benchmark		
	0.97		Constant mean benchmark		
1	0.97	HadCM3BL	840 – 560	No ice – EAIS	Open – Open
2	1.08	HadCM3BL	840 – 840	No ice – EAIS	Closed – Closed
3	1.10	HadCM3BL	560 – 560	No ice – EAIS	Closed – Closed
4	1.17	HadCM3BL	560 – 560	No ice – EAIS	Open – Open
5	1.22	HadCM3BL	840 – 840	No ice – EAIS	Open – Open
			Late Eocene absolute + EOT change + Early Oligocene absolute		
	1.61		Latitudinal gradient benchmark		
1	2.06	HadCM3BL	840 – 840	No ice – EAIS	Open – Open
2	2.13	HadCM3BL	840 – 560	No ice – EAIS	Open – Open
3	2.41	HadCM3BL	560 – 560	No ice – EAIS	Open – Open
	2.77		Constant mean benchmark		
4	2.92	FOAM	1,120 – 560	No ice – small EAIS	Open – Open
5	2.94	FOAM	1,120 – 560	No ice –EAIS	Open – Open

4 Discussion

4.1 Plausible forcings of EOT climatic change

This model-data comparison shows that the most realistic representation of the high latitude Southern Hemisphere climate before, after and across the EOT would be simulated by an expansion of an AIS, possibly with some combination of

5 atmospheric pCO$_2$ decline. However, there is still clear room to improve the models' performance relative to the data. For the late Eocene and early Oligocene, generally the models provide a better representation of the relative spatial patterns of temperature (i.e. for the normalised RMSE metric) compared to the absolute temperatures (i.e. for the standard RMSE metric). Given that the simulations were run with relatively arbitrary orbital configurations and pCO$_2$ levels (although they are of a plausible magnitude; Pearson et al., 2009; Pagani et al., 2011; Foster et al., 2017), it is perhaps unsurprising that the absolute

10 temperature values are not a good fit for the data. It could be possible to attempt to scale the modelled temperature assuming a linear fit between the few pCO$_2$ levels simulated here; however, this would still provide just a simple approximation of the climate as it would not account for non-linear responses. A more rigorous model-data comparison would vary the pCO$_2$ levels by more subtle increments, but this would require significantly greater computing resources.

However, despite these limitations in the modelled absolute temperature before and after the EOT, incorporating this

15 information into the comparison influences which simulation pairs are identified as best at representing how the climate might have changed across the EOT. Without accounting for the absolute data, simulation pairs with a closed Drake Passage can perform well, whereas for the absolute data these simulations perform poorly.

The marked reduction in performance by HadCM3BL when the Drake Passage either is closed before and after the EOT or is closed before but opens across the EOT supports the conclusions of Goldner et al. (2014) that changes in ocean gateways

20 around the EOT are not the best way to model the changes observed in the proxy record. This is in support of the general shift in consensus away from the gateway hypothesis as the sole cause of the changes at the EOT, at least in terms of the direct climatic implications (DeConto & Pollard, 2003; Huber & Nof, 2006; Sijp et al., 2011; Ladant et al., 2014 etc.). However, a pre-conditioning by gateway deepening and invigorated Antarctic Circumpolar Current is still plausible based on SST proxy data and microfossil distribution from directly prior the EOT (Houben et al., 2019). There is inconclusive evidence in the

25 literature for fundamental changes in the Drake Passage around the EOT (e.g. Lagabrielle et al., 2009 and references therein), in agreement with the Getech palaeogeographic reconstructions, which have the gateway open throughout the period (see the Lunt et al., 2016, Figure S1; Kennedy-Asser et al., 2019, Supplementary Figure 1). Proxy evidence and reconstructions suggest the Tasman Seaway deepened close to the EOT (e.g. Stickley et al., 2004; Scher et al., 2015, Houben et al., 2019) and this could be of interest to focus on with future model comparisons.

30 The better fit with proxy data by FOAM when the AIS is not at its full extent also would be consistent with the other glaciological evidence. Various sites around the Ross Sea showed the maximum AIS expansion occurring around ~32 Ma (e.g. Olivetti et al., 2015; Galeotti et al., 2016), significantly after the EOT, while sedimentological evidence from the Weddell Sea

suggests that region of West Antarctica was not fully glaciated until much more recently (~15 Ma; Huang et al., 2014). If this climatic fingerprint of a smaller AIS is robust, given that this signal already appears to be present in the data even with only limited site locations, there could be potential in future work to be able to constrain the extent of the AIS using only a climate model and proxy temperature records, which could then be used to independently verify other estimates from ice sheet

5 modelling or proxy estimates using $\delta^{18}O$.

HadCM3BL simulations with differing AIS extent boundary conditions (those with the Getech palaeogeographic reconstructions from Kennedy-Asser et al., 2019) also show a similar result, with simulations with a smaller EAIS fitting the data better (figure not shown). However, as was discussed in Kennedy-Asser et al., these simulations are potentially not fully spun-up and so they are not included in the analysis of this paper. It should be noted that the FOAM simulations have a

10 relatively short spin-up of 2,000 years (Table 1) and without deeper investigation into the time series of the model spin-up, it is not possible to say if this model is yet fully in equilibrium.

4.2 Changes in the latitudinal temperature gradient

A major concern identified in the model-data comparison is that the simulation pairs for both models do a poor job at recreating the change across the EOT compared to the latitudinal gradient benchmark or even the constant mean benchmark. This suggests

15 that these simulation pairs are having issues recreating the latitudinal profile of temperature change that is indicated by the data. The zonal mean temperature for each of the best pairs of simulations from HadCM3BL and FOAM (across all three time slices) are shown in Figure 3 along with the proxy records and their uncertainty.

Generally for the late Eocene, the latitudinal gradients produced by the models are reasonably similar to the gradient shown in the proxy records, although the models generally have a cold bias of around 5-10 °C (Figure 3a). As discussed previously,

20 however, it is unsurprising that there is some absolute bias as the pCO_2 levels used in the simulations are relatively arbitrary. For the early Oligocene, the models show an inflection in their latitudinal gradients around 65 °S (Figure 3b). Between 65-80 °S there is a steeper latitudinal gradient, which fits only with the relatively uncertain vegetation temperature reconstruction for the Ross Sea during this period (Raine & Askin, 2001). The S-index record for the Ross Sea suggests much warmer temperatures for the region (Passchier et al., 2013), which are close to the maximum limit of temperature for that latitude for

25 the HadCM3BL simulation, suggesting that this model does find some localised areas that are consistent with the data at that latitude.

The zonal mean of the modelled change in temperature across the EOT is very different from the proxies for both models, shown in Figure 3c. From 55-65 °S, the HadCM3BL and FOAM simulations are mostly in agreement with the mean change observed in the proxy records, however, in the models south of 65 °S there is a strong increase in cooling with poleward

30 latitude, again due to the cooling effect of the ice sheet, with a zonal mean cooling in the range of 10-15 °C at 75 °S. At the Ross Sea site, the S-index proxy suggests only minor cooling of 1 ±5 °C (Passchier et al., 2013). Although, the vegetation records could suggest greater cooling at this site, given the large range in early Oligocene temperature estimates from these

records (Francis & Hill, 1996; Raine & Askin, 2001; Passchier et al., 2013, supplementary information), it has not been possible to fully constrain the EOT temperature change with this data.

Critically assessing the proxy records that are included in the compilation could explain some of the differences between the records and the models. For example, it can be unclear as to what area the terrestrial proxies such as the S-index represent, or to what extent this record is affected by reworking. The S-index, like any detrital-based proxy, will suffer to some extent from reworking of older material (Passchier et al., 2013). This residual signal, primarily built up in warmer periods, implies that a warm-bias is likely. Additionally, although the dataset used here was as large as could be compiled at the time of writing, there are still large data gaps spatially and temporally. It is possible the sites around the Ross Sea are part of very localised microclimates, which may not align with the average climate of the large areas covered by a model grid cell.

A second option that could partly explain the model-data discrepancy is that local-regional scale warming signals in response to Antarctic glaciation due to enhanced circulation, deep water formation and sea ice feedbacks (as identified in models by Goldner et al., 2014; Knorr & Lohmann, 2014; Kennedy et al., 2015; Kennedy-Asser et al., 2019; and some of the FOAM simulations used here from Ladant et al. 2014; figure not shown) could be compensating for some of the cooling. When this warming is combined with a pCO$_2$ decline, the models do suggest that some very localised areas (i.e. < 5 grid cells) show little cooling or even warming, while other regions around the world cool more (figure not shown). It is therefore possible that the models are producing a qualitatively realistic result, however they do not get the location or magnitude to match the proxy datasets. A potential issue with this hypothesis is that the modelled warming with glaciation was shown in Kennedy-Asser et al. to be largely reduced with increasing spin-up, suggesting a similar effect could negate the at least some of the warming found in the other models (with the spin-up lengths of Goldner et al., 2014, Knorr & Lohmann, 2014 and Ladant et al., 2014 all ranging between 2,000-3,500 years).

Another significant model-data discrepancy is the strong cooling indicated by U$^{K'}_{37}$ at the Falklands Plateau (Liu et al., 2009; Plancq et al., 2014), which is significantly greater than any cooling recorded at any other Southern Ocean site or at any other site in the Atlantic more broadly (Liu et al., 2009). Although the most recent TEX$_{86}^{H}$ reconstructions suggest more moderate cooling, this could be biased towards summer temperatures (Houben et al., 2019), so the U$^{K'}_{37}$ record cannot be disregarded. This major cooling is hard to explain by any large-scale oceanic process. Even if there were to be a shift in the Antarctic Circumpolar Current and the Antarctic convergence, resulting in cold Southern Ocean waters reaching the site, surface waters 8 °C cooler lie more than 15 ° further south. As a result, the model simulations presented here would suggest that the major cooling that occurred at this site (assuming it is not due to some other error or bias in the record processing) is due to a geographically restricted (small scale) feature, such as becoming influenced by an upwelling of cold deep and/or intermediate water. Such features are below the resolution of these models and unfortunately cannot be expected to be captured.

A final important consideration is that the temporal averaging of the dataset carried out here could be inappropriate. A number of studies have suggested there was cooling in the several million years prior to the EOT, particularly at high latitudes (e.g. Raine & Askin, 2001; Petersen & Schrag, 2015; Passchier et al., 2016; Carter et al., 2017; Pound & Salzmann, 2017). Even in the high Northern Hemisphere changes have been identified occurring prior to the EOT (e.g. Coxall et al., 2018). These changes

5 could all have a range of different forcings; however, it is possible that some of them are related. Even a global forcing such as atmospheric pCO$_2$ decline would potentially have a signal that is detected first at higher latitudes. If there is polar amplification of the cooling signal and if there is a threshold of magnitude at which temperature changes could be identified in the proxy record (or other elements of the Earth system start to respond to the temperature change; e.g. changes in vegetation, weathering or precipitation), then even with a gradual decline in pCO$_2$ there could appear to be temporal heterogeneity in the

10 response.

Regardless of whether late Eocene cooling was earlier or simply amplified at higher latitudes, in both cases it is likely that the Ross Sea site experienced significant cooling prior to the EOT. This would support evidence of some tundra vegetation in the region recorded prior to the EOT (Raine & Askin, 2001). It therefore might be necessary to include older records and further

15 split the dataset into additional time slices to capture the climate of Antarctica before any cooling occurred. The only record of this age included in the current dataset is the McMurdo erratic, which suggested temperatures of less than 13 °C (Francis et al., 2009); however, the original location of this fossilised section is unknown and it could represent an area further south or at higher altitude, and thus introduce a cold temperature bias and is not suitable to use in isolation.

20 Currently, the data compilation is not big enough to allow for such analysis to be carried out; however, this could potentially offer a more appropriate comparison with the equilibrium climate model simulations used here, which are broadly 'warm and ice-free' or 'cool and glaciated'. If this hypothesis is correct, if more comparable records were included for the period pre-cooling and glaciation (e.g. dating from 40 Ma), it is possible that the high latitude change from the mid-late Eocene through to the Oligocene would be greater than that which is shown in Figure 3, closer in line with the model simulations.

5 Conclusions

An extensive review of temperature proxy records for the high latitude Southern Hemisphere region before, after and across the EOT was presented and used to evaluate model simulations of the EOT. These simulations came from two different GCMs with different sets of boundary conditions. The best simulations were able to capture spatial patterning of absolute temperature

30 recorded in the late Eocene and early Oligocene proxy datasets. The performances were not as good for the dataset of relative changes across the EOT, due to the models inadequately capturing changes in the latitudinal gradient shown by the data. The latitudinal gradients shown by the data are possibly related to the paucity of data in certain regions (particularly at very high

latitude), the time averaging of the proxy records into time slices (with some of the higher latitude changes possibly occurring prior to the EOT), localised climatic effects (e.g. ocean upwelling or ice free coastal microclimates) or possibly because the glaciation of Antarctica results in some localised warming through changes in atmospheric or oceanic circulation that approximately balances the general cooling across the EOT (e.g. due to pCO$_2$ decline). If the latter in the case, it would

5   qualitatively support the responses found by HadCM3BL and FOAM, as well as by other models (Goldner et al., 2014; Knorr & Lohmann, 2014). If this is correct, the poorer results in the model-data comparison carried out here may be because the models are simply mis-identifying the areas where the warming occurs.

The best pairs of simulations for modelling the absolute temperatures and relative changes were found by assessing the
10   individual simulations' performance across all time slices for various metrics. This suggests that the best simulations for representing the EOT were by HadCM3BL with an open Drake Passage, AIS expansion and possibly a drop in atmospheric pCO$_2$ levels. The poorer fit with the data for the late Eocene and early Oligocene when the Drake Passage is closed suggests the gateway was open for the duration of this period, while an opening of the Drake Passage across the EOT also produces a poor fit with the various datasets compiled here. This suggests the Drake Passage was open prior to the late Eocene and EOT
15   and so opening of the Drake Passage was an unlikely driver of the EOT (in agreement with the results of DeConto & Pollard, 2003; Goldner et al., 2014 etc.).

The performance of FOAM for the early Oligocene time slice was better with smaller ice sheet configurations over Antarctica, potentially in agreement with proxy records of ice volume and extent (e.g. Bohaty et al., 2012; Huang et al., 2014; Galeotti et
20   al., 2016). A similar finding is also seen in the HadCM3BL simulations using the Getech palaeogeographies (not shown); however, as these simulations could be affected by a lack of spin-up, they were not included in the analysis. Further spinning-up those HadCM3BL simulations with multiple ice sheet sizes could provide some interesting insights into whether this climatic fingerprint of a smaller AIS is robust.

25   An important consideration in interpreting this model-data comparison is the relative paucity of data available for the region during the EOT, in combination with records generally showing heterogeneous temperature patterns. Particularly for the normalised RMSE, an important measure for determining if the model is showing the correct spatial patterns, there are only a handful of sites which can be used across all sectors of the Southern Ocean. With the relatively limited data coverage available here, it is possible that these latitudinal profiles could be biased by anomalous values. To attempt to account for this uncertainty,
30   this model-data comparison could be repeated, systematically omitting different sites or proxy data points. However, as noted in Section 2.4, this was done for the calculation of the latitudinal gradient in the change across the EOT, with a negative slope still persisting even with the extreme Falklands Plateau site omitted. Based on this provisional result, this kind of analysis would not be expected to fundamentally affect the model-data comparison across the EOT.

Future research by the palaeoclimate community will inevitably produce new records in new locations, potentially refining or even correcting older, spurious results or having an impact on the inferred spatial patterns shown in the proxy record. Future work on this research could improve the consistency of the data used, for example in terms of using the same proxy calibrations, age models and definitions of uncertainty, but that is currently beyond the scope of this paper. To this end, the datasets used

5   here have been uploaded to the Open Science Framework (Kennedy-Asser, 2019) to aid in the continuation of this research and the expansion of this analysis in the future. Additionally, future work can also expand upon this analysis by including more model simulations and trialling other metrics and scoring techniques. The challenge in synthesising the many changes that occurred in this large and heterogeneous region across the EOT is huge, but this research shows that with increased modelling and proxy data results, some convergence of ideas within the palaeoclimate community appears possible.

References

Baatsen, M.J.L., von der Heydt, A.S., Huber, M., Kliphuis, M.A., Bijl, P.K., Sluijs, A. & Dijkstra, H.A.: Equilibrium state and
5   sensitivity of the simulated middle-to-late Eocene climate, *Climate of the Past Discussions*, DOI: 10.5194/cp-2018-43, 2018.

Bohaty, S.M., Zachos, J.C. & Delaney, M.L.: Foraminiferal Mg/Ca evidence for Southern Ocean cooling across the Eocene-
Oligocene transition, *Earth and Planetary Science Letters*, 317-318, pp. 251-261, DOI: 10.1016/j.epsl.2011.11.037, 2012.

Carter, A., Riley, T.R., Hillenbrand, C.D. & Rittner, M.: Widespread Antarctic glaciation during the Late Eocene, *Earth and
Planetary Science Letters*, 458, pp. 49-57, DOI: 10.1016/j.epsl.2016.10.045, 2017.

10   Coxall, H.K. & Pearson, P.N.: The Eocene-Oligocene transition, in Williams, M., Hayward, A., Gregory, J., and Schmidt, D.
N., eds., Deep time perspectives on climate change: Marrying the signal from computer models and biological proxies:
London, Geological Society Publishing House, p. 351-387, 2007.

Coxall, H.K., Wilson, P.A., Pälike, H., Lear, C.H. & Backman, J.: Rapid stepwise onset of Antarctic glaciation and deeper
calcite compensation in the Pacific Ocean, *Nature*, 433, pp. 53-57, DOI: 10.1038/nature03135, 2005.

15   Coxall, H.K., Huck, C.E., Huber, M., Lear, C.H., Legarda-Lisarri, A., O'Regan, M., Sliwinska, K.K., van de Flierdt, T., de
Boer, A.M., Zachos, J.C. & Backman, J.: Export of nutrient rich Northern Component Water preceded early Oligocene
Antarctic glaciation, *Nature Geoscience*, 11, pp. 190-196, DOI: 10.1038/s41561-018-0069-9, 2018.

DeConto, R. M. & Pollard, D.: Rapid Cenozoic glaciation of Antarctica induced by declining atmospheric CO_2, *Nature*, 421,
pp. 245-249, 2003.

20   Dowsett, H.J., Robinson, M.M., Haywood, A.M., Hill, D.J., Dolan, A.M., Stoll, D.K., Chan, W.L., Abe-Ouchi, A., Chandler,
M.A., Rosenbloom, N.A., Otto-Bliesner, B.L., Bragg, F.J., Lunt, D.J., Foley, K.M. & Riesselman, C.R.: Assessing confidence
in Pliocene sea surface temperatures to evaluate predictive models, *Nature Climate Change*, 2, pp. 365-371, DOI:
10.1038/NCLIMATE1455, 2012.

Foster, G.L., Royer, D.L. & Lunt, D.J.: Future climate forcing potentially without precedent in the last 420 million years,
25   *Nature Communications*, 8:14845, DOI: 10.1038/ncomms14845, 2017.

Francis, J.S. & Hill, R.S.: Fossil Plants from the Pliocene Sirius Group, Transantarctic Mountains: Evidence for Climate from
Growth Rings and Fossil Leaves, *Palaios*, 11, 4, pp. 389-396, 1996.

Francis, J.E., Marenssi, S., Levy, R., Hambrey, M, Thorn, V.T., Mohr, B., Brinkhuis, H., Warnaar, J., Zachos, J.C., Bohaty,
S.M., & DeConto, R.M.: From Greenhouse to Icehouse – The Eocene/Oligocene in Antarctica. In: Developments in Earth &
30   Environmental Sciences, 8, F. Florindo and M. Siegert (Editors), DOI 10.1016/S1571-9197(08)00008-6, 2009.

Galeotti, S., DeConto, R.M., Naish, T., Stocchi, P., Florindo, F., Pagani, M., Barrett, P., Bohaty, S.M., Lanci, L., Pollard, D., Sandroni, S., Talarico, F.M. & Zachos, J.C.: Antarctic Ice Sheet variability across the Eocene-Oligocene boundary climate transition, *Science*, 352, 6281, pp. 76-80, DOI: 10.1126/science.aab0669, 2016.

Goldner, A., Herold, N. & Huber, M.: Atlantic glaciation caused ocean circulation changes at the Eocene-Oligocene

5   transition, *Nature*, 511, pp. 574-577, DOI: 10.1038/nature13597, 2014.

Houben, A.J.P., Bijl, P.K., Pross, J., Bohaty, S.M., Passchier, S., Stickley, C.E., Röhl, U., Sugisaki, S., Tauxe, L., van de Flierdt, T., Olney, M., Sangiorgi, F., Sluijs, A., Escutia, C., Brinkhuis, H.A. & the Expedition 318 Scientists: Reorganization of Southern Ocean Plankton Ecosystem at the Onset of Antarctic Glaciation, *Science*, 340, pp. 341-344, DOI: 10.1126/science.1223646, 2013.

10   Houben, A. J. P., Bijl, P. K., Sluijs, A., Schouten, S. & Brinkhuis, H.: Late Eocene Southern Ocean cooling and invigoration of circulation preconditioned Antarctica for full-scale glaciation, *Geochemistry, Geophysics, Geosystems*, 20, pp. 2214–2234. DOI: 10.1029/2019GC008182, 2019.

Huang, X., Gohl, K. & Jokat, W.: Variability in Cenozoic sedimentation and paleo-water depths of the Weddell Sea basin related to pre-glacial and glacial conditions of Antarctica, *Global and Planetary Change*, 118, pp. 25-41, DOI:

15   10.1016/j.gloplacha.2014.03.010, 2014.

Huber, M. & Caballero, R.: The early Eocene equable climate problem revisited, *Climate of the Past*, Volume 7, pp. 603-633, DOI: 10.5194/cp-7-603-2011, 2011.

Huber, M. & Nof, D.: The ocean circulation in the southern hemisphere and its climatic impacts in the Eocene, *Palaeogeography, Palaeoclimatology, Palaeoecology*, 231, pp. 9-28, 2006.

20   Hutchinson, D.K., de Boer, A.M., Coxall, H.K., Caballero, R., Nilsson, J. & Baatsen, M.J.L.: Climate sensitivity and meridional overturning circulation in the late Eocene using GFDL CM2.1, *Climate of the Past,* Volume 14, pp. 789-810, DOI: 10.5194/cp-14-789-2018, 2018.

Kennedy A.T., Farnsworth A., Lunt D.J., Lear C.H., & Markwick P.J.: Atmospheric and oceanic impacts of Antarctic glaciation across the Eocene–Oligocene transition, *Phil. Trans. R. Soc. A*, 373, 20140419, DOI:10.1098/rsta.2014.0419,

25   2015.

Kennedy-Asser, A.T., Lunt, D.J., Farnsworth, A. & Valdes, P.J: Assessing mechanisms and uncertainty in modelled climatic change at the Eocene-Oligocene Transition, *Paleoceanography and Paleoclimatology*, 34, pp. 16-34, DOI: 10.1029/2018PA003380, 2019.

Kennedy-Asser, A. T.: EOT_SOcean (accessed 29th August 2019), https://doi.org/10.17605/OSF.IO/BKN26, 2019.

30   Knorr, G. & Lohmann, G.: Climate warming during Antarctic ice sheet expansion at the Middle Miocene transition, *Nature Geoscience*, 7, pp. 376-381, DOI: 10.1038/ngeo2119, 2014.

Ladant, J.B., Donnadieu, Y., Lefebvre, V. & Dumas, C.: The respective role of atmospheric carbon dioxide and orbital parameters on ice sheet evolution at the Eocene-Oligocene transition, *Paleoceanography*, DOI: 10.1002/2013PA002593, 2014.

Lagabrielle, Y., Goddéris, Y., Donnadieu, Y., Malavieille, J. & Suarez, M.: The tectonic history of Drake Passage and its possible impacts on global climate, *Earth and Planetary Science Letters*, 279, pp. 197-211, DOI: 10.1016/j.epsl.2008.12.037, 2009.

Liu, Z., Pagani, M., Zinniker, D., DeConto, R., Huber, M., Brinkhuis, H., Shah, S.R., Leckie, R.M., & Pearson, A.: Global

5 cooling during the Eocene–Oligocene climate transition, *Science*, 323, pp. 1187-1190, DOI: 10.1126/science.1166368, 2009.

Lunt, D.J., Dunkley Jones, T., Heinemann, M., Huber, M., LeGrande, A., Winguth, A., Lopston, C., Marotzke, J., Roberts, D.C., Tindall, J., Valdes, P.J. & Winguth, C.: A model–data comparison for a multi-model ensemble of early Eocene atmosphere–ocean simulations: EoMIP, *Climate of the Past*, 8, pp. 1717-1736, DOI :1 0.5194/cp-8-1717-2012, 2012.

Lunt, D. J., Farnsworth, A., Lopston, C., Foster, G.L., Markwick, PJ., O'Brien, C.L., Pancost, R.D., Robinson, S.A. & Wrobel,

10 N. Palaeogeographic controls on climate and proxy interpretation, *Climate of the Past*, 12, pp. 1181-1198, DOI: 10.5194/cp-12-1181-2016, 2016.

Nooteboom P. D., Bijl, P. K., van Sebille, E., von der Heydt, A.S. & Dijkstra, H. A.: Transport bias by ocean currents in sedimentary microplankton assemblages: Implications for paleoceanographic reconstructions, *Paleoceanography and Paleoclimatology*, 34, DOI: 10.1029/2019PA003606, 2019.

15 Olivetti, V., Balestrieri, M.L., Rossetti, F., Thomson, S.N., Talarico, F.M. & Zattin, M.: Evidence of a full West Antarctic Ice Sheet back to the early Oligocene: insight from double dating of detrital apatites in Ross Sea sediments, *Terra Novai*, pp. 238-246, DOI: 10.1111/ter.12153, 2015.

Pagani, M., Huber, M., Liu, Z., Bohaty, S.M., Henderiks, J., Sijp, W., Krishnan, R. & DeConto, R.M.: The Role of Carbon Dioxide During the Onset of Antarctic Glaciation, *Science*, 334, pp. 1261-1264, DOI: 10.1126/science.1203909, 2011.

20 Passchier, S., Bohaty, S.M., Jiménez-Espejo, F., Pross, J., Röhl, U., van de Flierdt, T., Escutia, C. & Brinkhuis, H.: Early Eocene to middle Miocene cooling and aridification of East Antarctica, *Geochemistry, Geophysics, Geosystems*, 14, 5, pp. 1399-1410, DOI: 10.1002/ggge.20106, 2013.

Passchier, S., Ciarletta, D.J., Miriagos, T.E., Bijl, P.K. & Bohaty, S.M.: An Antarctic stratigraphic record of stepwise ice growth through the Eocene-Oligocene transition, *GSA Bulletin*, DOI: 10.1130/B31482.1, 2016.

25 Pearson, P.N., Foster, G.L., & Wade, B.S.: Atmospheric carbon dioxide through the Eocene-Oligocene climate transition, *Nature*, 461, pp. 1110-1113, DOI: 10.1038/nature08447, 2009.

Petersen, S.V. & Schrag, D.P.: Antarctic ice growth before and after the Eocene-Oligocene transition: New estimates from clumped isotope paleothermometry, *Paleoceanography*, 30, pp. 1305-1317, DOI: 10.1002/2014PA002769, 2015.

Plancq, J., Mattioli, E., Pittet, B., Simon, L. & Grossi, V.: Productivity and sea-surface temperature changes recorded during

30 the late Eocene–early Oligocene at DSDP Site 511 (South Atlantic), *Palaeogeography, Palaeoclimatology, Palaeoecology*, 407, pp. 34-44, DOI: 10.1016/j.palaeo.2014.04.016, 2014.

Pound, M.J. & Salzmann, U.: Heterogeneity in global vegetation and terrestrial climate change during the late Eocene to early Oligocene transition, *Scientific Reports*, 7, p. 43386, DOI: 10.1038/srep43386, 2017.

Raine, J.I. & Askin, R.A.: Terrestrial Palynology of Cape Roberts Project Drillhole CRP-3, Victoria Land Basin, Antarctica, *Terra Antarctica*, 8, pp. 389-400, 2001.

Scher, H.D., Bohaty, S.M., Smith, B.W. & Munn, G.H.: Isotopic interrogation of a suspected late Eocene glaciation, *Paleoceanography*, 29, pp. 628-644, DOI: 10.1002/2014PA002648, 2014.

Scher, H.D., Whitaker, J.M., Williams, S.E., Latimer, J.C., Kordesch, W.E.C. & Delaney, M.L.: Onset of Antarctic Circumpolar Current 30 million years ago as Tasmanian Gateway aligned with westerlies, *Nature*, 523, pp. 580-583, DOI: 10.1038/nature14598, 2015.

Sijp, W.P., England, M.H. & Huber, M. Effect of deepening the Tasman Gateway on the global ocean, *Paleoceanography*, 26, PA4207, DOI: 10.1029/2011PA002143, 2011.

Stickley, C.E., Brinkhuis, H., Schellenberg, S.A., Sluijs, A., Rohl, U., Fuller, M., Grauert, M., Huber, M., Warnaar, J. & Williams, G.L.: Timing and nature of the deepening of the Tasmanian Gateway, *Paleoceanography*, 19, PA4027, DOI: 10.1029/2004001022, 2004.

Villa, G., Fioroni, C., Persico, D., Roberts, A.P. & Florindo, F.: Middle Eocene to Late Oligocene Antarctic glaciation/deglaciation and Southern Ocean productivity, *Paleoceanography*, 29, pp. 223-237, DOI: 10.1002/2013PA002518, 2013.

Wilson, D.S., Pollard, D., DeConto, R.M., Jamieson, S.S.R. & Luyendyk, B.P.: Initiation of the West Antarctic Ice Sheet and estimates of total Antarctic ice volume in the earliest Oligocene, *Geophysical Research Letters*, 40, pp. 4305-4309, DOI: 10.1002/grl.50797, 2013.

Zachos, J.C., Shackleton, N.J., Revenaugh, J.S., Pälike, H. & Flower, B.P.: Trends, Rhythms, and Aberrations in Global Climate 65 Ma to Present, *Science*, 292, pp. 686-693, DOI: 10.1126/science.1059412, 2001.

Zonneveld, K.A.F., Marret, F., Versteegh, G.J.M., Bogus, K., Bonnet, S., Bouimetarhan, I., Crouch, E., de Vernal, A., Elshanawany, R., Edwards, L., Esper, O., Forke, S., Grøsfjeld, K., Henry, M., Holzwarth, U., Kielt, J.F., Kim, S.Y., Ladouceur, S., Ledu, D., Chen, L., Limoges, A., Londeix, L., Lu, S.H., Mahmoud, M.S., Marino, G., Matsouka, K., Matthiessen, J., Mildenhal, D.C., Mudie, P., Neil, H.L., Pospelova, V., Qi, Y., Radi, T., Richerol, T., Rochon, A., Sangiorgi, F., Solignac, S., Turon, J.L., Verleye, T., Wang, Y., Wang, Z. & Young, M.: Atlas of modern dinoflagellate cyst distribution based on 2405 data points, *Review of Palaeobotany and Palynology*, 191, pp. 1-197, DOI: 10.1016/j.revpalbo.2012.08.003, 2013.